ACS APPLIED ELECTRONIC MATERIALS

pubs.acs.org/acsaelm Article

Electron-Beam Direct Writing-Based High-Performance Graphene Electrode Fabrication

Kaicheng Yu, Hao Tian, Rui Li, Luzhen Hao, Kaimin Zhang, Xiaodong Zhu, Yanqing Ma, and Lei Ma*

Cite This: https://doi.org/10.1021/acsaelm.3c00917 Read Online

ACCESS | Metrics & More | Article Recommendations | Supporting Information

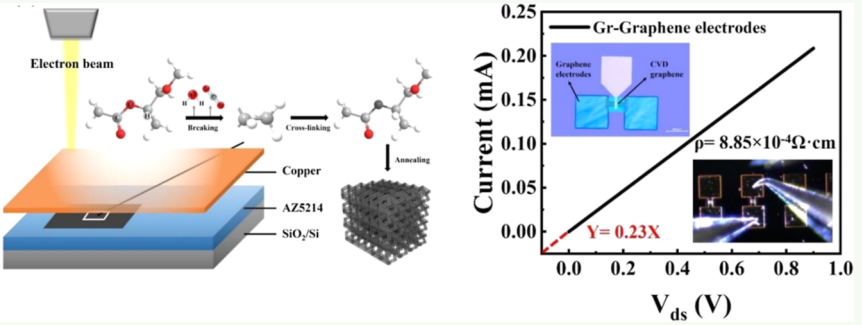

ABSTRACT: Graphene has attracted intensive attention in the field of nanoelectronics due to its excellent electrical, thermal, and mechanical properties, and graphene-based electronic devices emerge endlessly. However, with the miniaturization of devices and the improvement of circuit integration, the contact resistance between the metal electrode and graphene in the conventional graphene-based electronic devices largely reduces the carrier mobility and saturation drift speed due to the work function difference, which will greatly deteriorate the transport performance of the device. The high contact resistance can also cause device overheating and fast aging, consequently downgrading the upper bound of their performance. Therefore, hunting for an optimal electrode material and fabrication approach have been essential goals in the field. Here, we report a newly developed scheme that uses e-beam direct writing to make a high-performance three-dimensional graphene electrode, which can be applied in all carbon-based field effect transistors; the whole process was conducted in a hot filament scanning electron microscope. We systematically investigated all performance-processing parameter dependences and realized a resistivity of 8.85×10^{-4} Ω·cm of the graphene electrode, which has great application potential in developing all-carbon electronics.

KEYWORDS: *AZ5214, electron-beam-direct-writing, graphene electrode, three-dimensional, all-carbon electronics*

INTRODUCTION

Graphene is a two-dimensional material with excellent properties and broad prospects. It has been widely studied in the field of nanoelectronics because of its unique bipolarity and high carrier mobility.[1−3] Graphene-based electronic devices are considered as vital candidates for the postsilicon electronics.[4] Major conventional graphene electronics are made of metal−graphene−metal structures, where graphene serves as both channel and wires. However, the working function difference between the metal and graphene inevitably leads to the accumulation of a large amount of space charge on the interface between the two materials to generate a space charge field, consequently leading to the bending of the energy band and creating a so-called Schottky barrier. It creates an extra contact resistance in such a case,[5−7] which can seriously deteriorate the device performance.[8] Therefore, appropriate electrode material selection is of great significance for realizing the practical application of high-performance graphene electronics. Among them, the carbon-based electrodes are considered as potential alternatives to metallic ones due to their excellent thermal stability and possibly low working function difference to graphene and corrosion resistance comparing to metals.[9] Surely, a graphene-based electrode will be the ideal one. Much effort has already been made toward graphene-based all-carbon electronic devices. Park et al.[10] realized the selective growth of graphene and graphite and the control of the number of graphene layers using the patterning of heterogeneous metal catalysts, thus preparing a graphene transistor array with graphitic electrodes and interconnects. Chen et al.[11] reported a graphene-based field effect transistor, whose patterned fossil graphitic electrodes were fabricated by photolithography and oxygen plasma etching. Son et al.[12] have

Received: July 9, 2023
Accepted: August 28, 2023

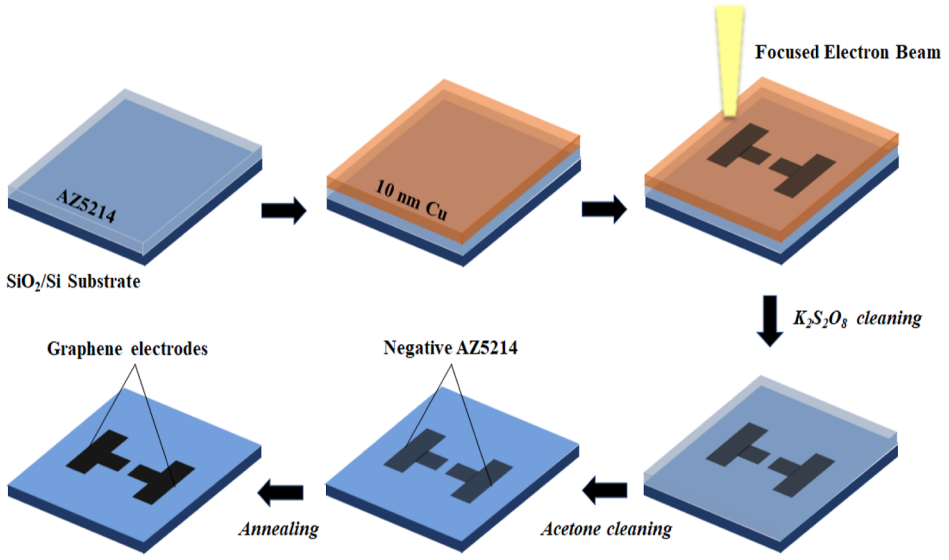

Figure 1. Flowchart of 3D graphene electrode fabrication.

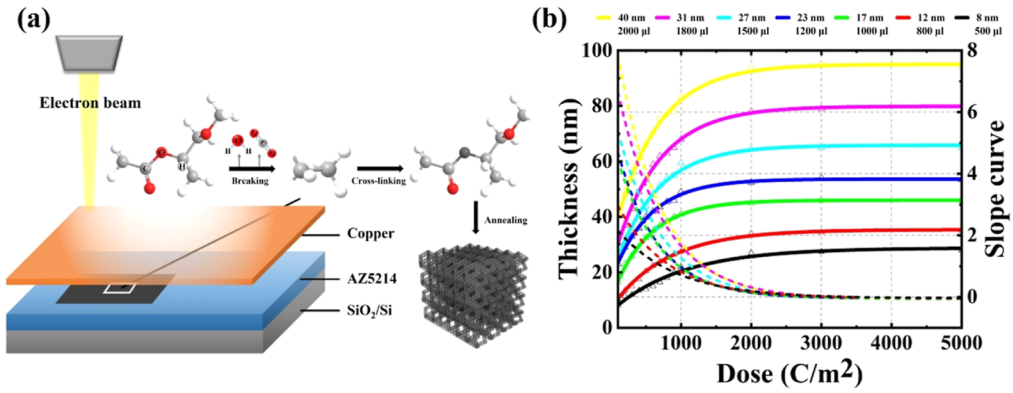

Figure 2. (a) Schematic illustration of the mechanism of 3D graphene electrode formation through e-beam direct writing using a photoresist. (b) The concentration and e-beam dose dependence of the thickness of graphene electrodes and the gradient of thickness change with beam dose increase. The label in the figure represents the concentration and the minimum electrode thickness corresponding to the concentration.

reported the process of graphene hydrogenation with hydrogen plasma and the scheme of converting the patterned fossil graphene into an all-graphene circuit recently.

Among the techniques for carbon-based electrode fabrication, e-beam direct writing is a very promising one due to its low power dissipation and nanoscale direct patterning capability,[13,14] which can fulfill the requirements for the fabrication of highly integrated electronics. Besides, it can avoid most of the steps in conventional lithography-based techniques, thereby greatly improving the fabrication efficiency and power usage. Conductivity and stability are two key criteria to evaluate the potential performance of an electrode material, and much work on seeking the best materials has been conducted with keen interest in those two in the past decade. McDermott et al.[15] prepared a conductive carbon nanostructure by combining e-beam direct writing and carbonization. During e-beam irradiation, with the carbonization of polymer, amorphous carbon forms, and the final resistivity of the graphitic layer was about 1.08×10^{-3} Ω·cm. Later, Chen et al.[9] reported a back-gate field effect transistor with graphitic electrodes fabricated by e-beam direct writing on polymethylmethacrylate (PMMA); the resistivity of graphitic electrodes was 4.8×10^{-3} Ω·cm, but the huge resistance (10^6 Ω) between source and drain electrodes remains an unsolved problem in its way to be applied practically.

Here, we report a newly developed scheme that can succeed in making a high-performance three-dimensional (3D) graphene electrode by scanning electron microscope e-beam direct writing with a photoresist AZ5214 thin film[16] and applying to an all-carbon-based top-gate field-effect transistor. The formed 3D graphene electrodes show a resistivity of 8.85 $\times 10^{-4}$ Ω·cm, and fabricated transistors having on-state source leakage electrode resistance of about 4.3 kΩ are comparable with the one made of conventional metallic electrodes.

METHODS AND EXPERIMENTS

Figure 1 illustrates the flowchart of 3D graphene electrode fabrication. Initially, diluted AZ5214 was spin-coated on the surface of a SiO_2/Si substrate [the rotating speed is 4000 revolutions per second (rps), and time is 40 s]. Then, a 5 nm thick copper film formed on its top as the catalyst layer through electron-beam evaporation deposition. The results showed that copper can largely enhance the breakage of C−C and C−H bonds in the photoresist molecule during e-beam irradiation.[17,18] The electron beam irradiation was conducted using a scanning electron microscopy system with a beam

https://doi.org/10.1021/acsaelm.3c00917
ACS Appl. Electron. Mater. XXXX, XXX, XXX−XXX

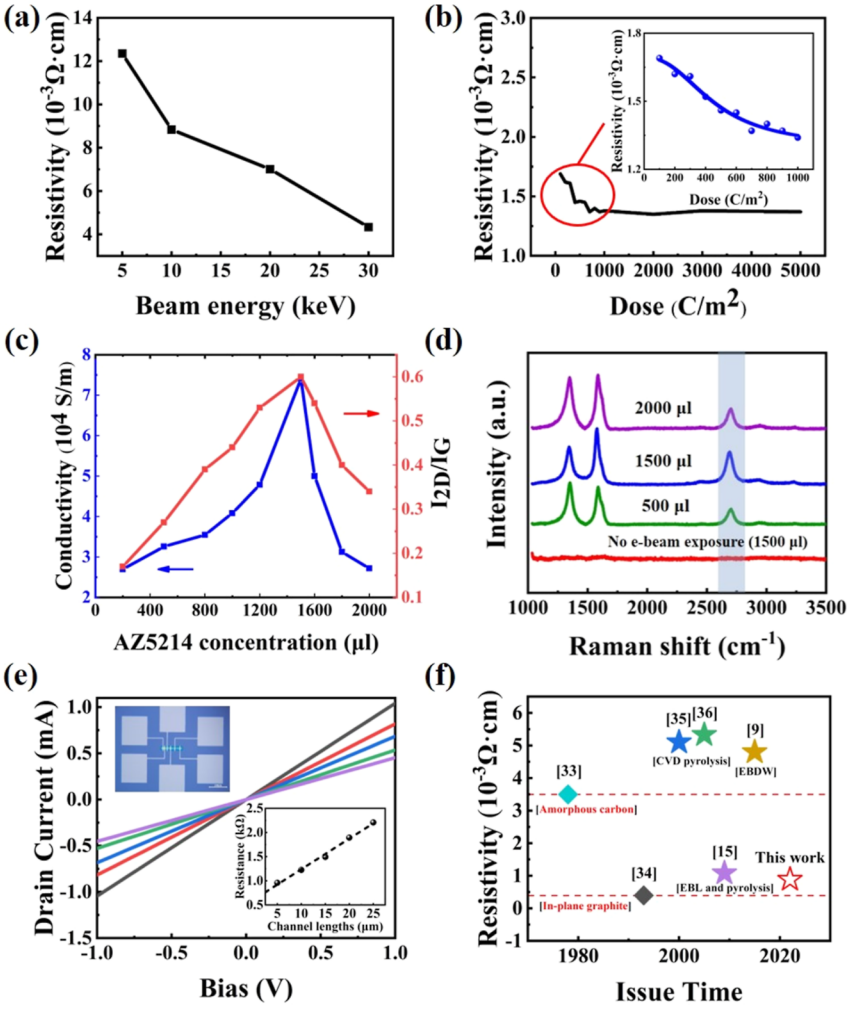

Figure 3. (a) Resistivity of the graphene electrodes under different beam energies. (b) Resistivity of the graphene electrodes under different electron irradiation doses. (c) Conductivity and I_{2D}/I_G of graphene electrode dependence on the concentration of photoresist for spin-coating. The horizontal coordinate represents the volume of AZ5214 dissolved in 20 mL of isopropyl alcohol. (d) Raman spectra measured for the grown graphene electrodes using the spin-coated films with different photoresist concentrations. The wavelength of the irradiated laser was 532 nm (e) Measured $I-V$ relationship of the GFET with channel lengths of 5, 10, 15, 20, and 25 μm; the inset is the plots of total resistances versus channel lengths. (f) Resistivity of reported graphitic electrodes prepared by different methods. (EBDW is e-beam direct writing; EBL is e-beam lithography; CVD is chemical vapor deposition).

energy of 5−30 keV. After that, the sample was soaked in potassium persulfate solution to remove the copper layer, and then, acetone was used to dissolve the unexposed resist so that the patterned parts were left. Finally, the sample was annealed at 800 °C for 1 h with the protection of Ar. The sample characterization was conducted using an atomic force microscope (NX-10, Park), a Raman spectrometer (RTS-2, with spectrometer Andor 500), and a probe station (Qianye probe station with Keithley model 2450) for thickness and surface roughness measurement, graphitic material recognition, and electric transport property measurements, respectively.

RESULTS AND DISCUSSION

Mechanism of 3D Graphene Electrode Fabrication. The fabrication of graphene electrodes by e-beam direct writing mainly includes two consecutive processes, electron beam irradiation or e-beam exposure and postannealing, as shown in Figure 2a.

The AZ5214 hydrocarbon is irradiated by a high-intensity electron beam that turns the large molecular chains into the small molecular carbon chains and then recross-link to form negative photoresist, producing a predefined 3D skeleton by losing part of oxygen and hydrogen atoms.[19,20] This is a typical overexposure process of positive photoresist.[21] Similarly, limited by the maximum voltage of the scanning electron microscope, the electron beam energy is insufficient to fully graphitize the precursor. The subsequent annealing process leads to a large number of cross-linked carbon−carbon bonds and dehydrogenization, and at the same time, the hydrogen and oxygen combination of volatile groups, such as CO_2, H_2, and CH_3O, escapes. The structure is expanded, and finally, a 3D graphene structure is formed with high electrical conductivity.[22,23]

Figure 2b shows that the thickness of the graphene electrodes increases initially and quickly reaches constant values with the increase of electron doses. The thickness increase of the irradiated resist is one of the key factors which later highly influence the 3D structure formation. Meanwhile, the high concentration of the precursor will lead to the high density of molecular chains; therefore, the thick 3D skeleton

https://doi.org/10.1021/acsaelm.3c00917
ACS Appl. Electron. Mater. XXXX, XXX, XXX−XXX

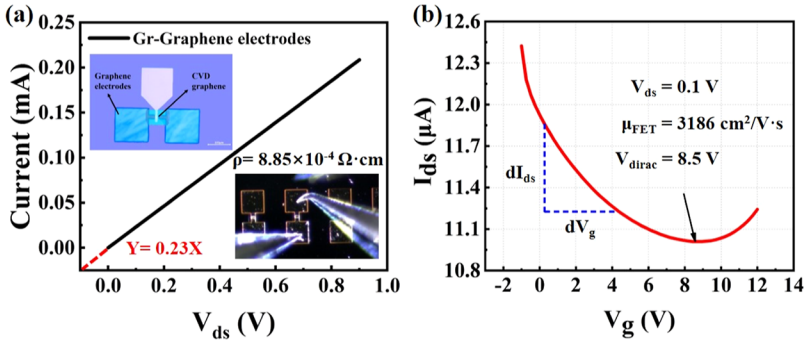

Figure 4. (a) Optical microscopic image and $I-V$ characteristic of 3D graphene electrode-based FET. The dielectric layer is a 30 nm Al_2O_3 layer deposited by atomic layer deposition. (b) Transfer characteristics of the GFET.

structure was formed after electron-beam irradiation and postannealing eventually.

Parameter Dependences of the Graphene Electrode Performance. To gain a deeper understanding of this technique, the parameter dependences of the graphene electrode performance were investigated systematically. The beam acceleration voltage or beam energy and dose are two of the most important parameters. The beam energy determines the maximum energy with which an electron can dissipate to the resist molecule.[24] As shown in Figure 3a, the resistivity of the fabricated material decreases with the increase in the beam energy. The collisions between the incident electrons and the molecules of the precursor result in the kinetic energy transfer of electron to the precursor molecule and lead to their fragmentation;[25] subsequently, the fragments cross-link and form a larger molecule with specific size distribution that is determined by both beam energy and dose. The whole process coincides with the typical process of overexposure of the positive photoresist.[26] Additionally, the resistivity of the electrode rapidly decreases with the increase in the beam dose,[27] but it will keep constant when the dose reaches or exceeds 1000 C/m^2, as shown in Figure 3b. The incident electrons induced high stress inside the resist, causing local plastic deformation. The aforementioned process leads to the positive to negative photoresist conversion, also a carbonation process,[28] and generates a predefined 3D skeleton, which prepares the needed precursors for the formation of a 3D graphene network in the following thermal annealing step.[29] The key to the optimization in this step is to seek the best parameters to obtain the most proper size distribution of negative photoresist and predefined deformation, which are favored for forming the right 3D graphene with both the lowest resistivity and the lowest annealing temperature required.

As shown in Figure 3c, with the increase of the concentration of the precursor solvent, the electrical conductivity of the electrode initially increases and then decreases and reaches the maximum value when the content of AZ5214 is 1500 μL. This could be interpreted as the maximization of positive to negative photoresist conversion (PVPC) and the optimized predefined structure for thermal carbonization to form 3D graphene under the same beam dose and energy. Under the same electron dose, the low-concentration resist solution-coated layer eventually leads to the formation of a thinner layer of 3D graphene, and consequently, the higher resistance, while too much resist may result in an unfavorable predefined structure for later 3D graphene network formation due to the incomplete PVPC.

Figure 3d shows the Raman spectrum of the resist-based electrode. A clear 2D characteristic peak formed at 2700 cm^{-1} indicates the critical feature of the multilayered graphene of the electrode for all electron irradiated electrodes but not for the one with solely annealing and without electron irradiation, which indirectly exhibits the significance of copper catalysis in graphene growth.[30−32]

Figure 3e shows the channel resistances of the fabricated electrodes with channel lengths of 5, 10, 15, 20, and 25 μm under the optimal fabrication parameters. Their nearly perfect linearity in $I-V$ curves indicates the great uniformity of the electrode materials and a resistivity of 8.85 × 10^{-4} Ω·cm. As shown in Figure 3f, it is the lowest among all the reported results in respect of materials and is an order of magnitude lower than that measured for the graphene electrode so far.[9,15,33−36]

Fabrication of 3D Graphene Electrode-Based FET. In order to further check the availability of this method, a 3D graphene electrode-based top-gate FET has been fabricated as shown in Figure 4a, where a piece of chemical vapor deposition (CVD)-grown graphene was transferred onto SiO_2/Si substrate as the channel material.[37] The perfect linear on-state $I-V$ relationship and nearly zero intercept indicate the low contact resistance between the electrode and graphene channel, which again indirectly prove the intrinsic nature of the fabricated electrode in the 3D graphene network. The measured on-state resistance is 4.3 kΩ, which coincides with the measured resistivity within the order of 10^{-4} Ω·cm.[9,15,38−40] In Figure 4b, the P-type device character is exhibited by the +8.5 V shift of the neutral point in the measured transfer curve of the top-gate FET. It could rationally be attributed to the photoresist residue on the graphene surface, which was introduced in the device patterning process. The reason for the curve rounding around the Dirac point is due to the defects in graphene, which can be attributed to the top fabrication of the electrode.[41] The extracted carrier mobility of the FET is 3186 cm^2/V s.[42] All of these demonstrate the scheme's fulfillment of the requirements of fabricating the electrodes for an all-carbon-based FET manufacture.

CONCLUSIONS

In this study, a high-performance 3D graphene electrode was successfully fabricated using AZ5214 by e-beam direct writing in the proposed scheme. Systematic studies of the electric property dependences of the manufactured electrode on a variety of fabrication parameters have been conducted, which include beam energy and dose and precursor concentration.

https://doi.org/10.1021/acsaelm.3c00917
ACS Appl. Electron. Mater. XXXX, XXX, XXX−XXX

The 3D graphene electrode with a resistivity of 8.85×10^{-4} Ω·cm was realized under the optimized condition, and the device exhibits no contact resistance, denoting the capability of its practical application. This photoresist-based scheme of nanoscale direct electrode fabrication has merits of rather high conductivity, zero graphene contact resistance, and simplicity compared to both the conventional metal and existing carbon-based electrodes for graphene electronics, which offers a highly promising tool in the arsenal of developing future all-carbon circuits.

■ ASSOCIATED CONTENT

Supporting Information

The Supporting Information is available free of charge at https://pubs.acs.org/doi/10.1021/acsaelm.3c00917.

Measurement of resistivity of the graphene electrode; resultant electrode with or without a copper layer for electron beam irradiation; and characterization of the directly annealed AZ5214 precursor without electron beam irradiation (PDF)

■ AUTHOR INFORMATION

Corresponding Author

Lei Ma − *Tianjin International Center for Nanoparticles and Nanosystems, Tianjin University, Tianjin, China 300072;* orcid.org/0000-0002-2446-4833; Email: Lei.ma@tju.edu.cn

Authors

Kaicheng Yu − *Tianjin International Center for Nanoparticles and Nanosystems, Tianjin University, Tianjin, China 300072*

Hao Tian − *Tianjin International Center for Nanoparticles and Nanosystems, Tianjin University, Tianjin, China 300072*

Rui Li − *Tianjin International Center for Nanoparticles and Nanosystems, Tianjin University, Tianjin, China 300072*

Luzhen Hao − *Tianjin International Center for Nanoparticles and Nanosystems, Tianjin University, Tianjin, China 300072*

Kaimin Zhang − *Tianjin International Center for Nanoparticles and Nanosystems, Tianjin University, Tianjin, China 300072*

Xiaodong Zhu − *Tianjin International Center for Nanoparticles and Nanosystems, Tianjin University, Tianjin, China 300072*

Yanqing Ma − *Tianjin International Center for Nanoparticles and Nanosystems, Tianjin University, Tianjin, China 300072; School of Precision Instrument and Optoelectronics Engineering, Tianjin University, Tianjin, China 300072;* orcid.org/0000-0002-3317-8273

Complete contact information is available at: https://pubs.acs.org/10.1021/acsaelm.3c00917

Author Contributions

K.Y and H.T contributed equally to this paper. L.M and Y.M. supervised the project. L.M. conceived and designed the experiments. K. Y. performed the experiments of 3D graphene electrode fabrication and characterization of materials. H.T. applied the electrodes to GFET. R.L., L.H., K.Z., and X.Z. analyzed the data and discussed the results. K.Y. wrote the manuscript. L.M and Y.M. revised and edited the manuscript. All the authors contributed to the manuscript preparation.

Notes

The authors declare no competing financial interest.

■ ACKNOWLEDGMENTS

The authors acknowledge the financial support from the National Key R&D Program of China (no. 2020YFC2004602).

■ REFERENCES

(1) Kong, W.; Kum, H.; Bae, S.-H.; Shim, J.; Kim, H.; Kong, L.; Meng, Y.; Wang, K.; Kim, C.; Kim, J. Path towards graphene commercialization from lab to market. *Nat. Nanotechnol.* **2019**, *14* (10), 927−938.

(2) Fakih, I.; Durnan, O.; Mahvash, F.; Napal, I.; Centeno, A.; Zurutuza, A.; Yargeau, V.; Szkopek, T. Selective ion sensing with high resolution large area graphene field effect transistor arrays. *Nat. Commun.* **2020**, *11* (1), 3226.

(3) Berger, C.; Song, Z. M.; Li, T. B.; Li, X. B.; Ogbazghi, A. Y.; Feng, R.; Dai, Z. T.; Marchenkov, A. N.; Conrad, E. H.; First, P. N.; de Heer, W. A. Ultrathin epitaxial graphite: 2D electron gas properties and a route toward graphene-based nanoelectronics. *J. Phys. Chem. B* **2004**, *108* (52), 19912−19916.

(4) Chhowalla, M.; Jena, D.; Zhang, H. Two-dimensional semiconductors for transistors. *Nat. Rev. Mater.* **2016**, *1* (11), 16052.

(5) Das, S.; Chen, H. Y.; Penumatcha, A. V.; Appenzeller, J. High performance multilayer MoS_2 transistors with scandium contacts. *Nano Lett.* **2013**, *13* (1), 100−105.

(6) Allain, A.; Kang, J. H.; Banerjee, K.; Kis, A. Electrical contacts to two-dimensional semiconductors. *Nat. Mater.* **2015**, *14* (12), 1195−1205.

(7) Di, C. A.; Wei, D. C.; Yu, G.; Liu, Y. Q.; Guo, Y. L.; Zhu, D. B. Patterned Graphene as Source/Drain Electrodes for Bottom-Contact Organic Field-Effect Transistors. *Adv. Mater.* **2008**, *20* (17), 3289−3293.

(8) Zhao, P.; Zhang, Q.; Jena, D.; Koswatta, S. O. Influence of metal-graphene contact on the operation and scalability of graphene field-effect transistors. *IEEE Trans. Electron Devices* **2011**, *58* (9), 3170−3178.

(9) Chen, W.; Yu, Y. Y.; Zheng, X. M.; Qin, S. Q.; Wang, F. H.; Fang, J. Y.; Wang, G.; Wang, C. C.; Wang, L.; Peng, G.; Zhang, X. A. All-carbon based graphene field effect transistor with graphitic electrodes fabricated by e-beam direct writing on PMMA. *Sci. Rep.* **2015**, *5* (1), 12198.

(10) Park, J.-U.; Nam, S.; Lee, M.-S.; Lieber, C. M. Synthesis of monolithic graphene-graphite integrated electronics. *Nat. Mater.* **2012**, *11* (2), 120−125.

(11) Chen, Z. P.; Narita, A.; Müllen, K. Graphene nanoribbons: on-surface synthesis and integration into electronic devices. *Adv. Mater.* **2020**, *32* (45), 2001893.

(12) Son, J.; Cha, J.; Hong, J. Electrical Patterning of Graphene Circuitry by Hydrogenation for Transparent and Flexible Devices. *Chem. Mater.* **2021**, *33* (2), 574−579.

(13) Dorp, W. F. v.; Hagen, C. W. A critical literature review of focused electron beam induced deposition. *J. Appl. Phys.* **2008**, *104* (8), 081301.

(14) de Boer, G.; Dansberg, M.; Jager, R.; Peijster, J. J. M.; Slot, E.; Steenbrink, S. W. H. K.; Wieland, M. *MAPPER: Progress toward a High-Volume Manufacturing System*; SPIE, 2013; Vol. *8680*.

(15) Du, R.; Ssenyange, S.; Aktary, M.; McDermott, M. T. Fabrication and characterization of graphitic carbon nanostructures with controllable size, shape, and position. *Small* **2009**, *5* (10), 1162−1168.

(16) Škriniarová, J.; Pudiš, D.; Andok, R.; Lettrichová, I.; Uherek, F. Investigation of the AZ 5214E photoresist by the laser interference, EBDW and NSOM lithographies. *Appl. Surf. Sci.* **2017**, *395*, 226−231.

(17) Bi, K. X.; Mu, J. L.; Geng, W. P.; Mei, L. Y.; Zhou, S. Y.; Niu, Y. K.; Fu, W. X.; Tan, L. G.; Han, S. Q.; Chou, X. J. Reliable fabrication of graphene nanostructure based on e-beam irradiation of PMMA/copper composite structure. *Materials* **2021**, *14* (16), 4634.

(18) Gao, H.; Belova, V.; La Porta, F.; Cingolani, J. S.; Andersen, M.; Saedi, M.; Konovalov, O. V.; Jankowski, M.; Heenen, H. H.; Groot, I.

M. N.; Renaud, G.; Reuter, K. Graphene at liquid copper catalysts: atomic-scale agreement of experimental and first-principles adsorption height. *Advanced Science* **2022**, *9* (36), 2204684.
(19) Van Dorp, W. F.; van Someren, B.; Hagen, C. W.; Kruit, P.; Crozier, P. Approaching the resolution limit of nanometer-scale electron beam-induced deposition. *Nano Lett.* **2005**, *5*, 1303−1307.
(20) Randolph, S. J.; Fowlkes, J. D.; Rack, P. D. Focused, nanoscale electron-beam-induced deposition and etching. *Crit. Rev. Solid State Mater. Sci.* **2006**, *31* (3), 55−89.
(21) Kulkarni, D. D.; Rykaczewski, K.; Singamaneni, S.; Kim, S.; Fedorov, A. G.; Tsukruk, V. V. Thermally induced transformations of amorphous carbon nanostructures fabricated by electron beam induced deposition. *ACS Appl. Mater. Interfaces* **2011**, 3 (3), 710−720.
(22) Wang, S.; Ang, P. K.; Wang, Z. Q.; Tang, A. L. L.; Thong, J. T. L.; Loh, K. P. High mobility, printable, and solution-processed graphene electronics. *Nano Lett.* **2010**, *10* (1), 92−98.
(23) Broers, A. N.; Harper, J. M. E.; Molzen, W. W. 250-Å linewidths with PMMA electron resist. *Appl. Phys. Lett.* **1978**, *33* (5), 392−394.
(24) Dusevich, V. M.; Purk, J. H.; Eick, J. D. Choosing the right accelerating voltage for SEM (An introduction for beginners). *Microsc. Today* **2010**, *18* (1), 48−52.
(25) Wu, B.; Neureuther, A. R. Energy deposition and transfer in electron-beam lithography. *J. Vac. Sci. Technol., B: Microelectron. Nanometer Struct.–Process., Meas., Phenom.* **2001**, *19* (6), 2508−2511.
(26) Pandey, A.; Maity, S.; Murmu, K.; Middya, S.; Bandyopadhyay, D.; Gooh Pattader, P. S. Self-organization of random copolymers to nanopatterns by localized e-beam dosing. *Nanotechnology* **2021**, *32* (28), 285302.
(27) Hogstrom, K. R.; Mills, M. D.; Almond, P. R. Electron beam dose calculations. *Phys. Med. Biol.* **1981**, *26*, 445−459.
(28) Duan, H. G.; Zhao, J. G.; Zhang, Y. Z.; Xie, E. Q.; Han, L. Preparing patterned carbonaceous nanostructures directly by over-exposure of PMMA using electron-beam lithography. *Nanotechnology* **2009**, *20* (13), 135306.
(29) Han, S.; Li, N.; Song, Y.; Chen, L.; Liu, C.; Xi, M.; Yu, X.; Qin, Y.; Xu, T.; Ma, C.; Zhang, S.; Wang, Z. E-beam direct synthesis of macroscopic thick 3D porous graphene films. *Carbon* **2021**, *182*, 393−403.
(30) Tuinstra, F.; Koenig, J. L. Raman spectrum of graphite. *J. Chem. Phys.* **1970**, *53*, 1126−1130.
(31) Ferrari, A. C.; Robertson, J. Interpretation of Raman spectra of disordered and amorphous carbon. *Phys. Rev. B* **2000**, *61* (20), 14095−14107.
(32) Ferrari, A. C.; Meyer, J. C.; Scardaci, V.; Casiraghi, C.; Lazzeri, M.; Mauri, F.; Piscanec, S.; Jiang, D.; Novoselov, K. S.; Roth, S.; Geim, A. K. Raman spectrum of graphene and graphene layers. *Phys. Rev. Lett.* **2006**, *97* (18), 187401.
(33) Poduri, S. Theoretical modeling and analysis of ammonia gas sensing properties of vertically aligned multiwalled carbon nanotube resistive sensors and enhancing their sensitivity, M.Sc. Thesis, University of Kentucky, 2010
(34) Pierson, H. O. *Handbook of Carbon, Graphite, Diamond, and Fullerenes: Properties, Processing, and Applications*; Noyes Publications, 1993; Chapter 5, p 61.
(35) Ranganathan, S.; McCreery, R.; Majji, S. M.; Madou, M. Photoresist-Derived Carbon for Microelectromechanical Systems and Electrochemical Applications. *J. Electrochem. Soc.* **2000**, *147* (1), 277.
(36) Park, B. Y.; Taherabadi, L.; Wang, C.; Zoval, J.; Madou, M. J. Electrical Properties and Shrinkage of Carbonized Photoresist Films and the Implications for Carbon Microelectromechanical Systems Devices in Conductive Media. *J. Electrochem. Soc.* **2005**, *152* (12), J136.
(37) Weber, N.-E.; Binder, A.; Kettner, M.; Hirth, S.; Weitz, R. T.; Tomović, Ž. Metal-free synthesis of nanocrystalline graphene on insulating substrates by carbon dioxide-assisted chemical vapor deposition. *Carbon* **2017**, *112*, 201−207.
(38) Ji, X.; Zhang, J.; Wang, Y.; Qian, H.; Yu, Z. A theoretical model for metal-graphene contact resistance using a DFT-NEGF method. *Phys. Chem. Chem. Phys.* **2013**, *15* (41), 17883−17886.
(39) Stokbro, K.; Engelund, M.; Blom, A. Atomic-scale model for the contact resistance of the nickel-graphene interface. *Phys. Rev. B* **2012**, *85* (16), 165442.
(40) Cusati, T.; Fiori, G.; Gahoi, A.; Passi, V.; Lemme, M. C.; Fortunelli, A.; Iannaccone, G. Electrical properties of graphene-metal contacts. *Sci. Rep.* **2017**, *7* (1), 5109.
(41) Chen, J. H.; Jang, C.; Adam, S.; Fuhrer, M. S.; Williams, E. D.; Ishigami, M. Charged-impurity scattering in graphene. *Nat. Phys.* **2008**, *4* (5), 377−381.
(42) Li, H.; Zhu, Y.; Islam, M. S.; Rahman, M. A.; Walsh, K. B.; Koley, G. Graphene field effect transistors for highly sensitive and selective detection of K+ ions. *Sens. Actuators, B* **2017**, *253*, 759−765.

https://doi.org/10.1021/acsaelm.3c00917
ACS Appl. Electron. Mater. XXXX, XXX, XXX−XXX